Cold bosons in optical lattices: an exact diagonalization study

Author: David Raventós i Ribera
*Facultat de Física, Universitat de Barcelona, Diagonal 645, 08028 Barcelona, Spain.**

Advisor: Bruno Juliá-Díaz and Co-Advisor: Tobias Graß

Abstract: Experimental setups of cold atoms in optical lattices reproduce several quantum many-particle models, including the Bose-Hubbard model. We study this model by means of exact diagonalization. This model carries a superfluid to Mott insulator quantum phase transition. In order to characterize the phase transition, we have computed the ground state of the system and its overlap with the analytic expressions for the Mott insulator and superfluid states, its one-body density matrix, and its Von Neumann entropy. We have also studied the effect of setting an attractive bias potential in one site of the lattice at different strengths and also the strongly biased case in the repulsive regime. Finally, we have also explored the case with attractive on-site interactions, finding correlated states in the weakly attractive regime.

I. INTRODUCTION

In theoretical physics, the simulation of models has been a major tool to manage non-analytic and huge problems for decades. Nowadays, computers perform the majority of the simulations, working with transistors and shift registers. That kind of calculation machines are called classical, since the memories they use are deterministic.

Feynman pointed out in 1986 [1] that, for some quantum systems of interest, it might exist an experimental system that mimics those systems in a simpler way than a classical simulation. He called such a system "quantum simulator". This is mainly due to the fact that the necessary memory to store classically all the states of the required Hilbert space increases exponentially with the number of particles in the system.

The modern concept of quantum simulator is not exactly the same that Feynman thought. Whereas he discussed about "universal quantum simulators" as systems capable to do calculations in the same way that a computer does, nowadays, when we refer to a quantum simulator, we are thinking in an experimental setup. In order to study a physical model (not the physical phenomena), the simulation with those experimental setups consists in controlling the parameters of the theoretical model through some physical tunable properties of the experiment. In this way we can experimentally explore the predictions of the original theoretical model.

This kind of setups are very appreciated to realize experimentally some systems whose theoretical calculations are too hard to be computed classically. Although the Hilbert space could be efficiently restricted using some algorithms (clearly enumerated in [2]), all the classical algorithms used to simulate a quantum system break at a relatively low number of particles (compared with the thermodynamic limit). In contrast, a quantum simulator should be capable of reproducing the model with as many particles we can engineer.

Due to the complexity of condensed matter physics, theorists try to understand physical phenomena studying them with very simplified models which conserve the essential symmetries of the original problem. If a model is able to reproduce the physical phenomena (although being a huge computational problem), the main problem is to link the input parameters of the model with the physical properties of the system, and especially, the calculated processes with the underlaying physical mechanism. In order to understand these links in quantum systems, quantum simulators can be great tools.

In the recent years, the availability to manipulate small quantum systems with a few atoms has aimed at building such setups. The interactions between atoms can be engineered and also their kinetic properties. These quantum simulators have often been built to simulate Hubbard models. The Hubbard model was introduced by Hubbard [3] in 1963 to describe the behavior of electrons in a solid, but is has been generalized to systems of fermions, bosons and mixtures in periodic potentials.

The Bose-Hubbard model (BHM) is a Hamiltonian used to model particles following the Bose statistics. There exists many variations of it in order to reproduce many different phenomena. Fisher *et al.* [4] predicted in 1989 that the Bose-Hubbard Hamiltonian exhibits a phase transition from a superfluid to a Mott insulator as the interactions are increased. The origin of that phase transition is genuinely quantum, it takes place also at zero temperature. This model has been simulated in an experimental setup with cold atoms in optical lattices [5].

An optical lattice is an array of microscopic optical periodic potentials induced by AC Stark effect of interfering laser beams. The optical potentials are created by interfering counter-propagating lasers, which cause an oscillating electric field. An electron in an atom in the presence of the oscillating electric field attains a time-dependent dipole moment. Due to the dipole and the electric field, the electromagnetic energy undergoes a shift, which is a quadratic Stark effect with an oscillat-

* raventosrd@gmail.com

ing electric field. Then, the atoms are pushed towards the maximum or minimum intensity positions if the laser frequency is lesser or greater than the frequency of the closer atom transition, respectively (called red or blue detuning). Optical lattices allow for engineering the processes of the particles by tuning the depth of the optical potentials, that is, changing the intensity of the lasers. Optical lattices also have many advantages as experimental realizations of a theoretical lattice: the optical potentials can create practically arbitrary lattices, they are ideal (free of defects) and rigid (phonon excitations are not allowed). When the frequency of the laser coincides with an atomic internal transition, the optical lattice could act as a cooling trap. Optical lattices also allow to manage several-component atoms, using lasers with different polarizations in atoms with several spin-dependent internal states. See Ref. [6] for an extensive review about this topic.

The first setup able to perform a quantum simulator using cold atoms in optical lattices was proposed by Jaksch *et al.* [7] in 1998. It should transform a weakly interacting Bose gas into a Mott insulator (MI) by loading atoms into an optical lattice. The experimental setup was performed successfully by Greiner *et al.* [5] in 2002. The superfluid (SF) to MI is a highly celebrated quantum phase transition. An important feature of the MI is that it has a promising application to be used as initialization of quantum computer registers: In a MI phase, the particles remain localized without tunneling. Then, the well-defined number of particles in each position allows one to know faithfully the initial number of particles in a register.

This work is organized as follows. The BHM is introduced in Sec. II. In Sec. III are introduced the many-body properties of the system used to characterize its behavior. Mainly, these properties are the eigenvalues of the one body density matrix, and the populations of the Fock spaces. They allow us to discern if the system is condensed and to show its spatial correlations. Entropies in the way of the Von Neumann one have been defined in order to summarize important information about the system in a single scalar value. In Sec. IV, the most relevant computational details of the calculations are explained. In Sec. V, the U/t value at which the MI-SF phase transition takes place is obtained by a finite size scaling. The effect of an strong impurity in the lattice is also discussed. In Sec. VI, the attractive interaction regime is explored.

II. THE BOSE-HUBBARD MODEL

The Bose-Hubbard Model can involve many kind of processes, but the simplest non-trivial model is obtained by keeping only two terms: the hopping term, which allow the exchange of particles between the sites, related to the kinetic energy, and the on-site interaction term, which can be repulsive or attractive. This model is able to reproduce the MI-SF quantum phase transition. The Hamiltonian of the model, reads,

$$\hat{\mathcal{H}} = -\sum_{j\neq k}^{N_\mathrm{s}} t_{k,j}\hat{a}_j^\dagger \hat{a}_k + \frac{U}{2}\sum_{i=1}^{N_\mathrm{s}} \hat{n}_i(\hat{n}_i - 1), \tag{1}$$

where $\hat{a}_j^\dagger$ ($\hat{a}_j$) creates (annihilates) one particle in the jth site and $\hat{n}_i = \hat{a}_i^\dagger \hat{a}_i$ is the number of particles operator in the ith site, being N_s the number of sites. To study such problem for a fixed number of particles N, a convenient basis is given by the states of the Fock space restricted to N particles,

$$|\beta\rangle \equiv \left|n_1^\beta, n_2^\beta, \cdots, n_{N_\mathrm{s}}^\beta\right\rangle, \tag{2}$$

where n_i^β is the number of particles at the ith site in the state $|\beta\rangle$ and β is the labeling of the Fock states. Since the number of particles N in the system is fixed, n_i^β satisfies $\sum_i^{N_s} n_i^\beta = N$ for any state $|\beta\rangle$. Arbitrary states can be written in this orthogonal basis,

$$|\Phi\rangle = \sum_\beta^{N_\mathrm{bas}} c_\beta |\beta\rangle. \tag{3}$$

For total number of particles N and sites N_s there are N_bas Fock states in the basis. This number is the number of ways of placing N particles in N_s sites, so,

$$N_\mathrm{bas} = \binom{N + N_\mathrm{s} - 1}{N} = \frac{(N + N_\mathrm{s} - 1)!}{N_\mathrm{s}!\,(N-1)!}. \tag{4}$$

We have restricted the calculations to 1D and 2D squared lattices with nearest neighbor interaction. Several studies [8] prove that it is enough to keep the essential symmetries to reproduce the phase transition. Then, the only nonzero contributions to the sum of the hopping in Eq. (1) come from the neighboring pairs and $t_{k,j}$ is a constant, t.

III. QUANTUM MANY-BODY PROPERTIES

Due to the characteristics of the system, (quantum mechanics-governed and composed by several particles), the following magnitudes will be useful in order to characterize the many-body properties present in the system.

A. Fragmentation on the ultracold gas

The major phenomenon in this system is the condensation of the ultracold gas. The generalization of the concept of Bose-Einstein condensation to interacting systems was introduced by Penrose and Onsager [9, 10]. They

established a condensation criterion in terms of the one-body density matrix (OBDM),

$$\rho^{(1)}\left(\mathbf{r},\mathbf{r}'\right)=\left\langle\psi^{\dagger}\left(\mathbf{r}'\right)\psi\left(\mathbf{r}\right)\right\rangle, \tag{5}$$

where the field operator $\psi^{\dagger}$ creates a boson at position $\mathbf{r}$ and $\langle\cdots\rangle$ is the thermal average at temperature T. Since $\rho^{(1)}$ is a Hermitian matrix, it can be diagonalized. So, the eigenvalues of $\rho^{(1)}$ are the populations of orthogonal eigenstates. Then, the usual Bose-Einstein condensation occurs when there is one eigenvalue which scales with N (being N the number of particles in the system) while the rest of eigenvalues do not scale with N. In those systems, many of the bosons of the system, often a macroscopic number, are populating only one pure single-particle state, which is often called "macroscopic wave function". This kind of systems, with only one macroscopically populated state, have "*single condensates*".

The generalization of the Penrose-Onsager characterization to bosons with q internal degrees of freedom is due to Mueller *et al.* [11]. In a conventional uncondensed system, the particles are populating many different single-particle states being the number of possible states much larger than the number of particles in the system. Then, all the occupation numbers are $\sim\mathcal{O}(1)$. In a "*single condensates*", there is one eigenstate whose eigenvalue is $\sim\mathcal{O}(N)$, while the rest are $\sim\mathcal{O}(1)$. A fragmented system has $q>1$ eigenvalues $\sim\mathcal{O}(N)$, while the rest are $\sim\mathcal{O}(1)$. The easiest thought of a fragmented condensate is a condensed system whose GS has a degeneracy which is non-extensive with N.

So, the main way to find out if a given state is condensed involves the computation of the OBDM and its diagonalization in order to study the order of the populations of its eigenstates.

In second quantization, the definition of the OBDM $\rho_{k,l}$ of a state $|\Phi\rangle$ is,

$$\rho_{k,l}=\langle\Phi|\,\hat{a}_l^{\dagger}\hat{a}_k\,|\Phi\rangle\,. \tag{6}$$

But writing the state $|\Phi\rangle$ as in Eq. (3), we get explicitly,

$$\rho_{k,l}=\sum_{\alpha,\beta}^{N_{\mathrm{bas}}}c_{\alpha}^{*}c_{\beta}\,\langle\alpha|\,\hat{a}_l^{\dagger}\hat{a}_k\,|\beta\rangle. \tag{7}$$

From the diagonalization of the OBDM in an arbitrary basis, one obtains

$$\rho_{i,j}=n_i^{\mathrm{OBDM}}\delta_{i,j}, \tag{8}$$

where n_i^{OBDM} is the ith largest eigenvalue of the OBDM. In order to simplify the information given by the eigenvalues of the OBDM of a given state, we introduce an entropy based on the Von Neumann one, S_1, which will be used in the following. It is defined as,

$$S_1=-\sum_{i}^{N_{\mathrm{s}}}p_i\ln p_i. \tag{9}$$

being $p_i=n_i^{\mathrm{OBDM}}/N$ the normalized eigenvalues of the OBDM, instead of the ones of the density matrix. So, $\sum_i p_i=1$. The minimum of S_1 is 0 and it takes place when $p_i=\delta_{i,1}$. The entropy S_1 have a maximum which equals $\ln N_{\mathrm{s}}$ when $p_i=1/n,\forall i$. So, its maximum value corresponds to a uniform probability distribution, whereas the minimum corresponds to a Dirac-δ distribution. In all computations, that entropy has been divided by its maximum value, $\ln N_{\mathrm{s}}$, in order get a non-extensive quantity, bounded by 0 and 1.

The entropy S_1 is focused in the condensation, given by the Penrose-Onsager criterion. It allows us to show the degree of condensation of the particles as a function of U/t. When the value is 0, the system is condensed, whereas when it is $\ln N_{\mathrm{s}}$, it is completely uncondensed. When the value is the logarithm of a certain integer q, the state is fragmented in q states.

B. Spatial correlations

In order to obtain the correlations between the particles occupying different positions, we take advantage from the fact that our Fock basis is based on the spatial structure of the system. Then, we define a second entropy S,

$$S=-\sum_{\beta}^{N_{\mathrm{bas}}}|c_{\beta}|^2\ln|c_{\beta}|^2. \tag{10}$$

where c_β are the coefficients of the decomposition of a given state into the Fock basis $|\beta\rangle$, Eq. (3). This quantity allows to discuss the degree of clustering of the particles in the Fock space. So, in analogy with the populations of the condensate and fragmented states, we can use this entropy as a scalar which contains information about the whole distribution of populations of the Fock space.

Fixing the position of a particle, the available Fock space is restricted. It turns out that clustering around a state of our Fock space implies a certain degree of spatial correlation in the system. This is directly related to the space-based construction of the Fock basis. In the case of having two sites in the lattice, this entropy S coincides with the left-right bipartite entropy.

IV. NUMERICAL METHODS

Programing operations are not a minor amount of the work in quantum many body calculations via exact diagonalization. In order to manage the large algebraic operations necessary to do the calculations, the computer code has to be highly optimized. We only will point out that the states of the basis of the Fock space have to be labeled in a coherent way, in order to manage efficiently the action of the Hamiltonian on the states. Many of that kind of tricks are clearly explained in [12].

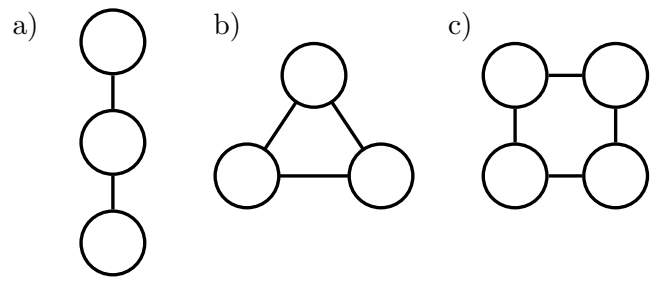

FIG. 1. a) 1D lattice with 3 sites and OBC. b) 1D lattice with 3 sites and PBC. c) 2D lattice with 2x2 sites and OBC or 1D lattice with 4 sites and PBC.

A. Finite lattices

The lattice has been defined labeling its sites with an index, from 1 to the number of sites, N_s. So, in the indexing of the sites, only one index will appear. However, it does not imply any restriction in the topology of the lattice.

Pointers are defined to manage the connections between the sites in the lattice. A pointer of a site is an array that lists all the sites connected with this site, according to its labels. If more than one kind of connections are needed, the pointers become matrices whose rows contain the labels with the same kind of interaction. For the case of the squared lattice with only nearest neighbor interactions, each pointer will have only one row with four labels (four neighbors and only one kind of interaction). One important point here is the existence of boundary conditions in the lattice, which are implemented in the definition of the pointers adding more labels corresponding to the neighbors behind the edge. We have done the calculations for a lattice with open and periodic boundary conditions (OBC and PBC, respectively).

Some examples of nearest neighbors lattices are shown in Fig. 1.

B. Exact diagonalization

The principal goal of this work is the exact diagonalization of Bose-Hubbard Hamiltonians. Given a lattice, a configuration of connections (including the geometry, the neighboring and the boundary conditions), and the values of the constants of the Hamiltonian, we can compute the action of the Hamiltonian on any state, which is a linear combination of the Fock states, Eq. (3),

$$\hat{\mathcal{H}}\,|\Phi\rangle = \sum_{\beta}^{N_\mathrm{bas}} c_\beta \hat{\mathcal{H}}\,|\beta\rangle\,. \tag{11}$$

Since the action of the Hamiltonian on an state is also a linear combination of Fock states, we can compute the whole Hamiltonian matrix in the Fock basis calculating the action of the Hamiltonian on the vectors of the Fock basis, $H_{\alpha,\beta} = \langle\alpha|\hat{\mathcal{H}}|\beta\rangle$. Diagonalizing the whole Hamiltonian matrix, we obtain the spectrum of the Hamiltonian and the GS and the excited states of the system decomposed in the Fock basis.

$N = N_\mathrm{s}$	N_bas
8	6435
10	92378
12	1352078

TABLE I. Number of particles at filling 1 and their corresponding size of the Fock space.

Here, we have constructed the Hamiltonian matrix (a complex $N_\mathrm{bas} \times N_\mathrm{bas}$ array), and then it has been diagonalized using the EISPACK package. It allows us to calculate in a reasonable time systems with $N_\mathrm{bas} \lesssim 3000$ in a desktop computer. This poses a strong restriction to the sizes considered, see Tab. I.

In order to save computer memory, the matrix could be saved sparse, since many elements of the Hamiltonian are zero. But the problem is not only the used memory, it is also the computation time in a crucial way. The complete diagonalization of a large matrix always is a difficult computational problem.

EISPACK package is unable to compute larger systems than the computed ones. But there are other ways to treat the problem. Since usually we are only interested in the GS and a few first excited states, it is not necessary to perform the whole matrix diagonalization. So, we could obtain only a few eigenvalues and its corresponding eigenvectors using an algorithm of power iteration with sparse storage.

V. MOTT INSULATOR TO SUPERFLUID TRANSITION

The Hamiltonian (1) exhibits two different quantum phases in the limit cases $t/U = 0, \infty$: a MI ground state and a SF phase.

A. Mott Insulator regime

When $t/U \to 0$ with $U > 0$, the system is ruled by the repulsive interactions, and it minimizes energy by reducing the number of pairs in each site. So, the GS of the system is a state with $q = N/N_\mathrm{s}$ particles on each site, where q is a positive integer, i. e., a Mott insulator state. This corresponds to one many-body state of the Fock basis and it reads,

$$|\Phi_\mathrm{MI}(q)\rangle = \prod_{i=1}^{N_\mathrm{s}} \frac{(\hat{a}_i^\dagger)^q}{\sqrt{q!}}\,|0\rangle = |q\cdots q\rangle\,. \tag{12}$$

The first excitation state looks like a MI state where a particle has been annihilated in one site and created in a different site, i. e., it is a quasiparticle-quasihole excitation of the MI state. When the particle is created in the ith site and the hole is localized in the jth one, the excited state reads as follows,

$$|\Phi_{\mathrm{MI}}(q)\rangle^{(1)} = \frac{1}{q}\hat{a}_i^\dagger \hat{a}_j \, |\Phi_{\mathrm{MI}}(q)\rangle \, . \tag{13}$$

The Mott insulator is an insulator in the sense that the "transport" of one particle from one site to another one costs a finite amount of energy (the energy gap ΔE). In the MI GS state, when q particles are in one site, the value of the interaction term in that site is $(U/2)q(q-1)$. When, in the MI state, a particle hop from one site to another, the value on the interaction term is $(U/2)(q-1)(q-2)$ in the site where the particle comes from and $(U/2)(q+1)q$ in the site where the particle goes. This situation coincides with the first excitation of the MI state. So, the energy difference of the MI state and its excitation is,

$$\begin{aligned} \Delta E &= \frac{U}{2}\left[(q-1)(q-2) + (q+1)q - 2q(q-1)\right] \\ &= U. \end{aligned} \tag{14}$$

So, the MI phase has a characteristic energy gap $\Delta E = U$ in the energy spectrum which separates the ground state from the excitations.

We will consider systems at filling factor, defined as $N/N_{\mathrm{s}} = 1$. This is the MI phase, there will be one particle in each site and $S_1 = \log N_{\mathrm{s}}$. Due to the fact that in this phase the GS coincides with a single Fock state, the second entropy S is zero. Since the number of particles q in each site is a well-defined integer, there are not fluctuations on the on-site number of particles in the Mott phase. The MI phase also has a finite correlation length.

B. Superfluid regime

When $U/t \to 0$, the hopping rules the system and each particle becomes completely delocalized over all sites of the lattice. So, we can write the single particle state as,

$$|\phi_{\mathrm{sp}}\rangle = \frac{1}{\sqrt{N_{\mathrm{s}}}} \sum_{i=1}^{N_{\mathrm{s}}} \hat{a}_i^\dagger \, |0\rangle \, . \tag{15}$$

Since there are not interactions, the state of the whole system is a properly symmetrized product of the single particle state up to the number of particles. So,

$$|\Phi_{\mathrm{SF}}\rangle = \frac{1}{\sqrt{N!}} \left[\frac{1}{\sqrt{N_{\mathrm{s}}}} \sum_{i=1}^{N_{\mathrm{s}}} \hat{a}_i^\dagger\right]^N |0\rangle \, . \tag{16}$$

Then, the squared coefficients of the decomposition of the SF state into the Fock basis follow a poissonian distribution in the sense that its variance $\mathrm{Var}\left(|c_\beta|^2\right)$ coincides with $\left\langle |c_\beta|^2 \right\rangle$ [5].

The SF state has the opposite properties to the MI state; it is characterized by a vanishing gap (since there is no interaction, the only contribution to the gap comes from the hopping term), large fluctuations in the on-site number of particles (since it is a pseudo-coherent state) and a divergent correlation function. In the SF phase, all the particles are maximally delocalized, that is, each one of them has the same probability of presence in all sites of the lattice, without interacting each other. Since all the particles in the system have the same single particle wavefunction, the system is condensed and so, the entropy S_1 as defined in Eq. (9), equals zero. In the SF phase, the entropy S_1 exhibits a minimum, since all the particles are in the same single-particle state, so, the system is condensed. Otherwise, the SF state involves many Fock states with a poissonian distribution, not uniform. The entropy S defined in Eq. (10), in the SF phase, will be larger than in the Mott phase, but it will never equals 1 because the distribution is not uniform. Actually, the value of the entropy S in the SF phase will decrease increasing the number of particles in the system, since the more particles in the system, the more differenced will be the values of the coefficients and the less uniform will be the distribution. In contrast to S_1, S does not exhibit an extremal value, since the distribution of coefficients could be more uniform in other cases, as shown in the subsec. VI A.

C. Quantum phase transition: Exact diagonalization results

Differently from the thermal phase transitions, due to the existence of an analytical solution of the system in the cases $U/t = 0, \infty$, we can compute the overlap of each solution with the GS found at a finite value U/t. This measure is a scalar that allows us to see a kind of likelihood of the ground state with a certain analytical state. It is the projection into the analytical state. In order for the value to make sense, both states are normalized to 1,

$$OV = \langle \Phi_{\mathrm{Analytic}} | \Phi_{\mathrm{GS}} \rangle \, . \tag{17}$$

We know the overlap of the analytic SF and MI states, which will be the limit of the GS of the system for $U/t = 0, \infty$, respectively. It is,

$$\langle \Phi_{\mathrm{MI}} | \Phi_{\mathrm{SF}} \rangle = \sqrt{\frac{N!}{(N_{\mathrm{s}})^N (q!)^{N_{\mathrm{s}}}}} = \sqrt{\frac{N!}{(N_{\mathrm{s}})^N (\frac{N}{N_{\mathrm{s}}}!)^{N_{\mathrm{s}}}}}. \tag{18}$$

For the kind of systems we are studying, $N_{\mathrm{s}} \lesssim N$, being $q = N/N_{\mathrm{s}}$ integer. For the case $q = 1$, $\lim_{N\to\infty} \sqrt{\frac{N!}{(N)^N}}$, and the overlap in Eq. (18) tends to 0.

In the overlap with the analytic SF state, see Fig. 2, all the states have overlap 1 at $U/t = 0$, as expected. For systems with different connectivity and the same N_{s}

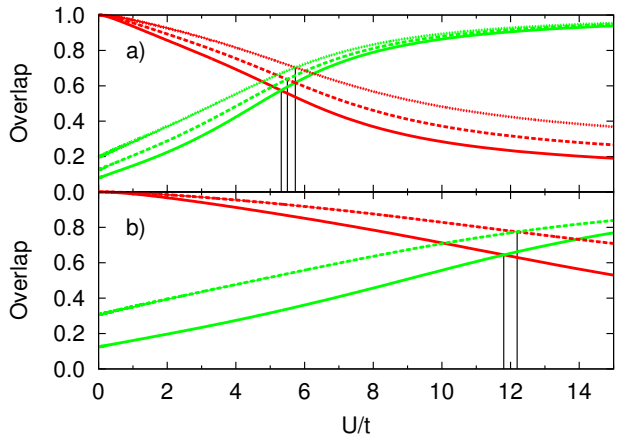

FIG. 2. a) Overlap of the GS of the system with the analytical SF (red) and MI (green) states in a 1D lattices with PBC and 5 (dotted line), 6 (dashed line) and 7 (solid line) sites. b) Computations in a 2D 2x2 (dashed line) and 3x2 (solid line) lattices with PBC are shown. The abscissa where the two overlaps have the same value is marked for easy visualization.

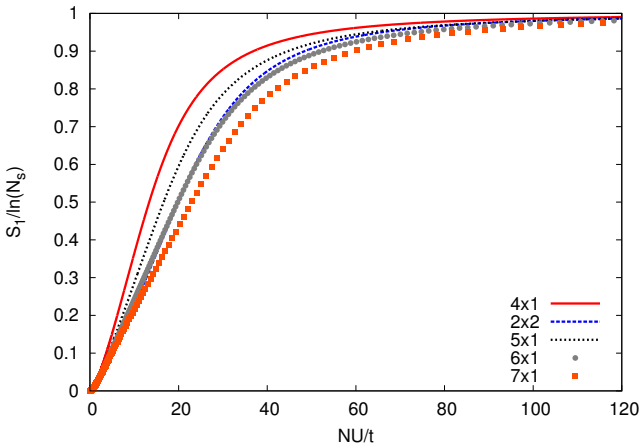

FIG. 3. Von Neumann entropy of the normalized eigenvalues of the OBDM of the GS of several systems with OBC.

(as example, 6×1 and 3×2, with PBC or OBS), the overlap of the GS and the analytic states goes to the same value (18) when $U/t \to 0, \infty$, due to the fact that the overlap between the analytic states does not depend on the connections, as expected.

The key difference between the two kind of boundary conditions considered is the connectivity of the edges. In both cases, the length of the system restricts the correlation length in the coherent states, but the PBC allow the system to be more connected. So, the SF phase survives at higher repulsion interaction with PBC than with OBC, whereas the MI phase become present in the system when the SF one vanishes.

Taking advantage from the fact that at $U/t = 0$ the system is in the SF phase and when $U/t \to \infty$ it is in the

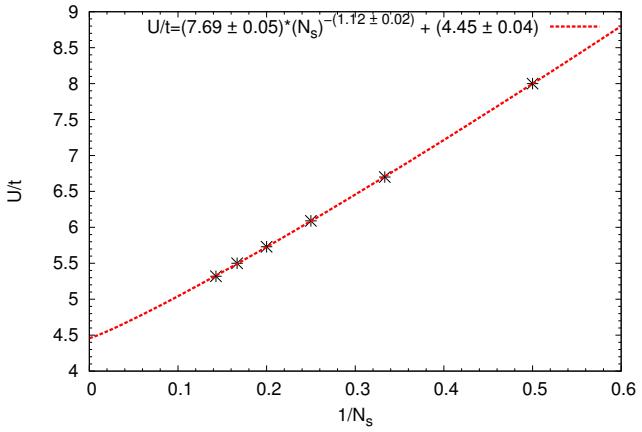

FIG. 4. U/t value where the phase transition takes place as function of the inverse size of the system $1/N_s$ in 1D systems with PBC. It is shown also the fitting to $U/t = a*(N_s)^{-b}+c$ made with the nonlinear least-squares Marquardt-Levenberg algorithm.

MI phase, for our finite system, we can use the overlap to define the U/t value where the phase transition takes place. Since the overlaps vary smoothly with U/t, it is easy to precisely find the intersection point. Note that in the thermodynamic limit the transition is sharp.

Given the size of the system, there is a certain U/t value, $(U/t)_{\mathrm{FS}}$, where the MI to SF phase transition takes place. Then, it is possible to perform a finite size study [13] to extrapolate the value at the thermodynamic limit, $(U/t)_{\mathrm{TL}}$. Since the expected dependency is $\left(\frac{U}{t}\right)_{\mathrm{FS}} = AN^{-b} + \left(\frac{U}{t}\right)_{\mathrm{TL}}$, a finite size study has been made for the 1D systems in Fig. 4.

The extrapolated value for the phase transition at the thermodynamic limit is $U/t = 4.45 \pm 0.04$ so, $t/U = 0.224 \pm 0.009$ with a reduced $\chi^2 = 6 \times 10^{-5}$. It agrees with the values in the literature [14]. Concretely, this value is placed in the Bose-Hubbard Hamiltonian phase diagram between the curve of the three-order strong-coupling expansion [15] and the curve from density-matrix renormalization-group calculations [16]. This accuracy could be expected, since we have exactly diagonalized the whole Hamiltonian without imposing any restriction on the Hilbert space and so, without losing any correlations. The only bad feature could be a slow convergence with the size to the thermodynamic value and the consequent wrong extrapolation.

D. Mott-Superfluid transition in a deep biased lattice

In any practical implementation of the finite size lattices considered there will be biases due to the imperfections. They can also be regarded as impurities in the system. In this section we study the role of an attractive potential on the GS properties.

In order to mimic an impurity, we can add a small attractive bias ϵ potential in the kth site. The way to do it is to add the term $-\epsilon \sum_i^{N_s} \hat{n}_i \delta_{i,k}$ in the Hamiltonian. This makes the system non-homogeneous.

To evaluate the effect of the bias potential in the system, we define the fluctuation of the number operator in the ith place,

$$(\Delta \hat{n}_i)^2 = \left\langle (\hat{a}_i^\dagger \hat{a}_i)^2 \right\rangle - \left\langle \hat{a}_i^\dagger \hat{a}_i \right\rangle^2. \tag{19}$$

It can be written explicitly with the number operators in the Fock basis. Moreover, due to the fact that the Fock states are eigenstates of $\hat{n}_i$, the only nonzero contribution occurs when $|\beta\rangle = |\alpha\rangle$. So,

$$(\Delta \hat{n}_i)^2 = \sum_\beta |c_\beta|^2 \langle \beta | \hat{n}_i | \beta \rangle^2 - \left[\sum_\beta |c_\beta|^2 \langle \beta | \hat{n}_i | \beta \rangle \right]^2. \tag{20}$$

The fluctuation of the on-site number of particles allows us to see how far away is a state from a phase transition which involves changes in the distribution of the particles in the states, for instance in MI to SF.

We have computed the fluctuation of the on-site number of particles in the biased site as function of U/t for given lattices and a given bias value. According to the properties of the SF and the MI: For small bias ϵ values ($\epsilon \ll t$ and $\epsilon \ll \Delta E$), the fluctuation is maximum in the SF phase. And it decreases upon increasing U/t, because in the deep repulsive regime and small bias ϵ, the number operator fluctuation vanish and the GS coincides very close with the MI phase.

For bias values $\epsilon \gtrsim t$, the fluctuation maximum is pushed to the repulsive regime, as shown in in Fig. 5. Increasing ϵ, there starts to appear maxima in the repulsion regime. The highest U/t value where there is a maximum coincides with ϵ/t.

When $\epsilon \gg t$, there are $N-1$ maximums in the strong repulsive regime, being N the number of particles in the system. In Fig. 5 we discuss in detail the case of a system with a single strongly biased state (with $\epsilon = 10^2 t$), There, the fluctuation of on-site number operator exhibits several maximums in the strongly repulsive regime. In order to infer which mechanisms produces them, we have calculated the population of each one of the sites in the lattice, simply taking the diagonal values of the OBDM and plotting them in Fig. 5. When the fluctuation reaches a maximum, the population in the biased site decreases by one, whereas in the other sites the population is increased depending on their position and the number of particles that have already gone out from the biased state. Between two consecutive fluctuation peaks, the populations remain mainly constant, showing plateaus with a step structure. When the maximum at highest U/t value is reached, the population of all the sites becomes the same integer value q and the fluctuation decrease monotonically, reaching the MI phase at $U/t \to 0$.

The population of each one of the sites in the lattice exhibits plateaus, shown in Fig. 5. The changes of the

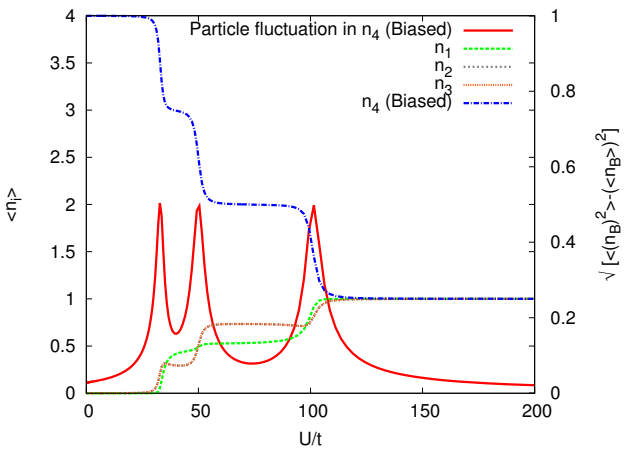

FIG. 5. Occupation numbers in a 2x2 lattice with OBC with a bias $\epsilon = 100t$ in the 4th site and fluctuation of the number operator in the biased site. The direct hopping between the 4th site and the 1st is not allowed and hopping between the 4th and the 2nd and 3rd are equivalent. The value of the bias $\epsilon = 100t$.

value of the plateau happen in the same values U/t and coincide with the maximums of the particle fluctuation in the 4th site (which is the biased one). So, they seem to be clearly related.

We can justify theoretically the U/t values in which a the fluctuation maxima appear. For the studied case, they are at $U/t = 33.33$, 50 and 100. These values are easily explainable for the MI with $q = 1$, keeping in mind the Hamiltonian in Eq. (1): the migration happens when the energy of keeping the particles in the same site become greater than the extracting of one particle from the biased site to place it in other site without particles,

$$\frac{U}{2} n_B(n_B - 1) - \epsilon n_B = \frac{U}{2}(n_B - 1)(n_B - 2) - \epsilon(n_B - 1), \tag{21}$$

where we have neglected the hopping term t due to the strong repulsion regime and the subindex B denotes the biased site. It leads us to the condition,

$$U = \frac{\epsilon}{n_B - 1}, \tag{22}$$

where n_B is a positive integer which $1 < n_B \leq N$.

The differences in the population of the different non-biased lattices are given by the connectivity of the lattice: when the interaction is large enough to push one particle from the biased site, the site which is not directly connected with the biased one is the second most populated. This is due to the fact that a particle should hop through two sites to find another one (it is farther from all other particles). Further increasing the energy, a second particle is pushed out, in this case, the two equivalent sites are more populated due to the fact that the two particles are avoiding being in the same unbiased site (are farther from each other).

As example, the same calculation in a 1D system with 3 sites, gives 2 equivalent non-biased sites if the system has OBC or the central site is biased in OBC, whereas it give two non-equivalent non-biased sites when, in OBC, the biased site is in one edge.

Essentially, the existence of a strong attracting bias incite the system to ignore the absence of the on-site U interaction, because the bias takes its place. Then, the particles do not acquire kinetic energy, as an insulator case, and so, the system avoids the SF phase.

An interesting future research could be to perform calculations with several topologies of the lattices and bias patterns in order to engineer connection-mediated phases.

VI. ATTRACTIVE INTERACTION: LOCALIZATION

We also studied the attractive case, $U < 0$. This case is often also studied in double-well potential systems, but not usually in optical lattices with many sites. It is due to the fact that the experimental setups involving optical lattices do not support attractive interactions. In fact, in the case of attractive interaction, more than two atoms are not allowed to be in the same site, due to the three-body loss [17]. The three-body loss is the loss of particles in a system due to the hard-core repulsive interaction occurring when a particle goes to a site already occupied by two more particles. The short-range repulsion between the three induces the loss of the particles.

For $U/t = -\infty$, all the particles in the system will aggregate in a single site so, the GS is the Fock state with N particles in the ith site and 0 in the other sites. But this state is N_s-degenerated. Due to this degeneration, there are N_s states which are superposed. Each one of them aggregates the system in one different site of the lattice. In this state, when a particle is fixed in one site, all the rest cluster there. So, this state is clearly correlated.

This perfect degeneracy is not found in the experimental setups, since there are many sources of inhomogeneities that lead to a single state GS. To control the kind of inhomogeneities, it is often set a controlled bias to manage the system. Here, the attractive bias ϵ favors the aggregation of the system in a site. This makes the system non-homogeneous, breaking the degeneracy and so, leading to a GS which is a single condensate. The localized condensate (LC) state in the kth site of the lattice, reads,

$$|\Psi_{\mathrm{LC}}(k)\rangle = \frac{1}{\sqrt{N!}}(\hat{a}_k^\dagger)^N |0\rangle \,. \tag{23}$$

In this state, as in the MI, the number of particles in each site is well defined and the correlation length vanishes, but the energy gap vanishes and its value is given by the value of the bias. Since this state is a single state of the Fock basis with all the particles localized in the same site, the values of the S_1 and S are both 0.

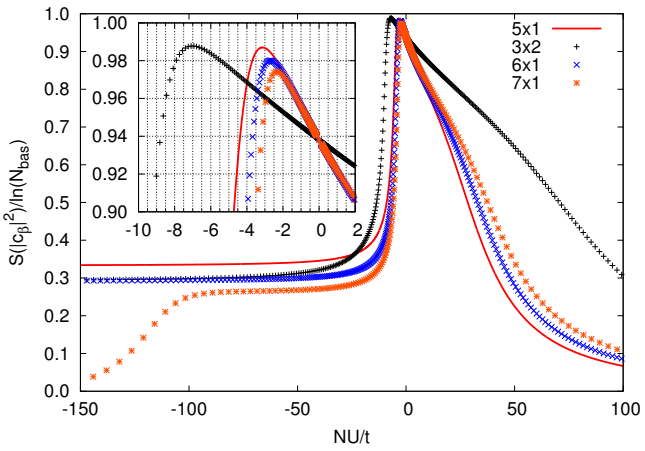

FIG. 6. Von Neumann entropy of the squared components of the linear decomposition of the GS into the Fock basis divided by $\ln N_{\mathrm{bas}}$. From 5 to 7 particles in several geometries of squared lattices and PBC. It is shown a zoom in order to appreciate the weakly attractive regime. Bias $\epsilon = 10^{-10}t$.

It is noticed that if several sites on the lattice were biased significantly more than the rest, it could be possible to obtain a fragmented condensate. It is also possible to engineer the number of fragmented fractions by setting a number of biased sites in the lattice.

A. Appearance of correlated states

The entropy S of several systems as function of NU/t in the attractive regime is depicted in Fig. 6. It has its maximum in the attractive regime, not at $U/t = 0$, differently from the minimum of the S_1. It is placed around $U/t \lesssim -1$ and it is closer to $U/t = 0$ when the size of the system increases, due to finite size effects. The only possible way to understand that is assuming that the distribution of coefficients of the GS at this U/t value is more uniform now that in the SF phase, at $U/t = 0$.

The phenomenon here is similar to the one given in Ref. [18] when the weakly attractive regime is performed. In that report, the system is a double-well where both, attractive and repulsive on-site interactions are allowed and it is performed under a small bias. That system coincides with the concrete case of the 1D lattice of two sites with OBC in our study. The basis of the Fock state is, $\{|N,0\rangle, |N-1,1\rangle, \ldots |N-k,k\rangle, \ldots, |0,N\rangle\}$ and is labeled with k. It becomes very useful in order to show the distribution of populations in the Fock space. Increasing the attraction from the non-interacting regime, the distribution of populations of the Fock space changes from a binomial distribution (due to the fact that the system have only two sites) to a one-peaked one around the localized state in the biased side in the strongly attractive regime (ruled by bias), thought a couple more: a plain distribution and a two-peaked one.

The way to understand the two-peaked distribution is

easy: the bias is much smaller than the energy gap and the GS becomes degenerate with two states, each one of them localize the system in one of the two sides. So, this state becomes a Schrödinger cat, which highly populates two different regions of the Fock space, keeping the rest of the Fock states unoccupied.

Then, there are two transitions: One, when the gap is small enough to let the bias break the left-right symmetry and rule the system, localizing the system in the biased site. This is, when the distribution changes from a two-peaked distribution to a one-peaked.

The other transition happens at lower on-site attraction values. This is, when there is a transition between the delocalized and uncorrelated superfluid phase and the localized and correlated cat-like state. The edge regions of the Fock space, the ones where all the particles are in the same site, are the least populated by the SF state, whereas they are the unique which are populated by the degenerate localized states. So, in this phase transition, the distribution of populations becomes highly uniform. Fig. 2. of Ref. [18] greatly clarifies the discussion.

What happens in the weakly attractive regime is that the bias is not large enough to rule the system to a LC state because the gap is too large. Then, the GS is almost degenerate. Then, the bosons in the system become correlated. In those correlated states, the distribution of population of the Fock states become more uniform than in the SF phase because the SF state favors the Fock states with maximally spatial dispersion (delocalization). In the state reached at that regime, there is a competition between the kinetic term that favors delocation, and the attraction interaction, that favors the spatial-aggregated states. This competition affects the distribution of populated Fock states, being more uniform. It is remarkable that, although there is a maximum of the entropy, the value does not reach its maximum possible value, thus, so, the distribution is not completely uniform in any case.

As the number of particles is increased the distribution is less uniform. It is more pronounced in the cases with OBC than in the PBC case. It is due to the natural bias induced by the hopping: the states which mostly populate the most connected sites are more probable than others (this is what happens in OBC). When all sites are equally connected, all equivalent states are equally probable (which is the situation in PBC).

B. Bias vs. attraction, localization

In the attractive regime, $U/t < 0$, the magnitude of the bias in a site (a impurity) becomes a control parameter to manage the appearance of correlated states when the bias $\epsilon \ll \Delta E$ at $U/t = 0$, the GS is almost degenerate, appearing degenerate states which localizes the system in a single site.

The gap ΔE in the spectrum of the system is the energy difference between the GS and the first excited state. It goes to 0 when the system remains in the LC phase.

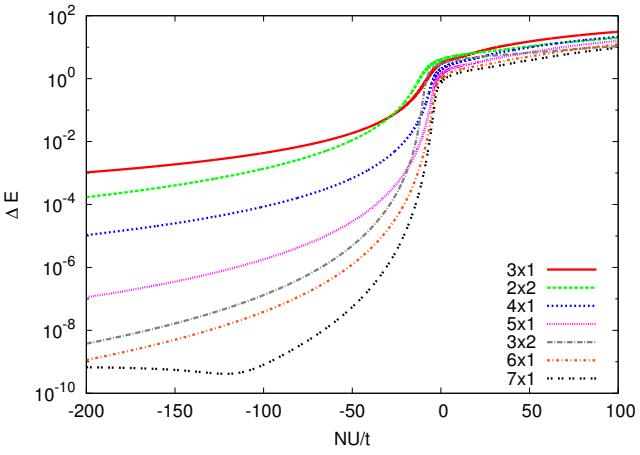

FIG. 7. Gap of several systems in squared lattice and with from 3 to 7 particles and with PBC. Bias $\epsilon = 10^{-10}t$.

In the MI phase, the gap exhibits a finite value which is linearly increasing with U/t. The gap should vanish in $U = 0$, but it has a finite value, as shown in Fig. 7. The bigger the system, the smaller the gap at fixed U/t, suggesting that the finite gap at $U = 0$ is a finite size effect.

The vanishing of the gap for $U/t < 0$ is quicker for the larger lattices than for the small ones. In Fig. 7 it is shown how the gap is limited by the machine resolution or by the bias.

In the region of the SF-MI phase transition ($U/t > 0$ and $U \sim t$), the gap exhibits a nonlinear dependency with U/t until the strong interaction regime is reached, due to the competition between t and U. Furthermore, the main difference between the results with different boundary conditions is essentially the following: the decay of the nonlinear behavior with U/t is faster in systems with OBC, due to the fact that the tunneling term of the Hamiltonian in the systems with PBC (with more connections) is larger.

If there is a strong bias, the correlated states shown in the attractive regime disappear, since the particles start to populate sites which are different from the biased one at a certain value of the repulsive interaction.

The topology of the lattice is not very important in the correlated states in the attractive regime because the only relevant quantity is the number of states in which the system can localize (which is the number of sites in the lattice).

VII. CONCLUSIONS & OUTLOOK

We have studied the exact ground state of atoms in optical lattices. Different regimes have been considered, ranging from the weakly-interacting superfluid regime, and even to the regime of attractive interactions, with localized GS. We have, found a way to define the Mott

insulator to superfluid transition as the parameter value for which the overlap of the ground state with both analytic states is equal. This of course only happens for finite systems, in the thermodynamic limit the overlap between the two states goes to zero. With such definition we have performed a finite size scaling to estimate the value of the MI to SF transition point. The found value is in agreement with previous estimates.

Many-body properties such as the condensed fraction or on-site particle fluctuations have been presented. In particular, we have studied how the latter depend on the value of the bias. An interesting feature appears when the bias is strong compared to the tunneling. In this case, as we increase the repulsive interactions, the ground state undergoes several transitions with large fluctuations of particle number in the transition region.

For the case of attractive interactions, we have studied the balance between the external bias and the attractive interaction. The interaction would imply a highly degenerate ground state, with a very small energy gap, e.g. cat states in double-well potentials. The bias, however, favors localization on one well. The bias dominates the system once it is larger than the energy gap.

A possible continuation here is the simulation of systems under magnetic field. Taking advantage from the Aharonov-Bohm effect [19] (the fact that a charged particle describing a closed loop under magnetic field acquires a non-vanishing phase proportional to the magnetic flux passing through the area enclosed by the loop), and from the fact that in concrete cases it is definite [20], a different phase can be given to a particle each time that it hops to sites in different directions (Ref. [21]), and therefore to different kinds of neighbors (Ref. [22]). It is a promising feature that can be implemented in the future in order to simulate Hall phases in lattices.

Another future direction could be the generalization of the problem to several components of bosons. The study of lattice gases in gauge fields is a promising topic encouraged by the possibility of experimental realization in the next few years. In this way, it would be exiting to show the competition of different insulator phases in the system. A topological insulator phase could be obtained in the way of Ref. [23] through the presence of magnetic field, whereas the Mott insulator one is induced by strong interactions at integer filling factor.

ACKNOWLEDGMENTS

I would like to thank Bruno Juliá-Díaz for his helpful work as tutor during the development of the technical stages of the project and for his revisions of this text, as well as for the enriching discussions with him. Likewise, I wish to thank Tobias Graß for his repeated revisions of the text and critical comments, as well as for sharing with me his broad vision on the field of study. I want to thank also the amazing discussions I enjoyed in the Cold Atoms Journal Club meetings. To perform this Master course, I was granted a scholarship from the Programa Màsters d'Excel·lència of the Fundació Catalunya-La Pedrera. Finally, I am also grateful to Iris Llop for her patience and support.

[1] R. Feynman, International Journal of Theoretical Physics **21**, 467 (1982).
[2] R. Orus, ArXiv e-prints (2013), arXiv:1306.2164 [cond-mat.str-el].
[3] J. Hubbard, Royal Society of London Proceedings Series A **276**, 238 (1963).
[4] M. P. A. Fisher, P. B. Weichman, G. Grinstein, and D. S. Fisher, Phys. Rev. B **40**, 546 (1989).
[5] M. Greiner, O. Mandel, T. Esslinger, T. W. Hansch, and I. Bloch, *Nature*, Nature **415**, 39 (2002).
[6] M. Lewenstein, A. Sanpera, and V. Ahufinger, *Ultracold Atoms in Optical Lattices: Simulating Quantum Many-body Systems* (OUP Oxford, 2012).
[7] D. Jaksch, C. Bruder, J. I. Cirac, C. W. Gardiner, and P. Zoller, Phys. Rev. Lett. **81**, 3108 (1998).
[8] A. M. Rey, *Ultracold bosonic atoms in optical lattices*, Ph.D. thesis, University of Maryland at College Park (2004).
[9] O. Penrose and L. Onsager, Phys. Rev. **104**, 576 (1956).
[10] O. Penrose, Philosophical Magazine Series 7 **42**, 1373 (1951).
[11] E. J. Mueller, T.-L. Ho, M. Ueda, and G. Baym, Phys. Rev. A **74**, 033612 (2006).
[12] J. M. Zhang and R. X. Dong, European Journal of Physics **31**, 591 (2010).
[13] M. Campostrini and E. Vicari, Phys. Rev. A **81**, 023606 (2010).
[14] F. E. A. dos Santos and A. Pelster, Phys. Rev. A **79**, 013614 (2009).
[15] J. K. Freericks and H. Monien, Phys. Rev. B **53**, 2691 (1996).
[16] G. G. Batrouni, R. T. Scalettar, and G. T. Zimanyi, Phys. Rev. Lett. **65**, 1765 (1990).
[17] P. O. Fedichev, M. W. Reynolds, and G. V. Shlyapnikov, Phys. Rev. Lett. **77**, 2921 (1996).
[18] B. Juliá-Díaz, D. Dagnino, M. Lewenstein, J. Martorell, and A. Polls, Phys. Rev. A **81**, 023615 (2010).
[19] Y. Aharonov and D. Bohm, Phys. Rev. **115**, 485 (1959).
[20] M. V. Berry, European Journal of Physics **1**, 240 (1980).
[21] M. Hafezi, A. S. Sørensen, E. Demler, and M. D. Lukin, Phys. Rev. A **76**, 023613 (2007).
[22] E. Kapit and E. Mueller, Phys. Rev. Lett. **105**, 215303 (2010).
[23] T. Graß, D. Raventós, M. Lewenstein, and B. Julià-Díaz, Phys. Rev. B **89**, 045114 (2014).